Since January 2020 Elsevier has created a COVID-19 resource centre with free information in English and Mandarin on the novel coronavirus COVID-19. The COVID-19 resource centre is hosted on Elsevier Connect, the company's public news and information website.

Talanta 245 (2022) 123482

Contents lists available at ScienceDirect

Talanta

journal homepage: www.elsevier.com/locate/talanta

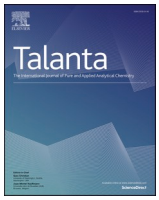

Electrochemical genosensor for the specific detection of SARS-CoV-2

Sebastian Cajigas [a], Daniel Alzate [a], Maritza Fernández [a], Carlos Muskus [b], Jahir Orozco [a,*]

[a] Max Planck Tandem Group in Nanobioengineering, Institute of Chemistry, Faculty of Natural and Exact Sciencies, University of Antioquia, Complejo Ruta N, Calle 67 N° 52–20, Medellín, 050010, Colombia

[b] Programa de Estudio y Control de Enfermedades Tropicales (PECET), Facultad de Medicina, Universidad de Antioquia, Calle 62 N° 52-59, Medellín, Colombia

ARTICLE INFO

Keywords:
Genosensor
SARS-CoV-2
Nanobioconjugate
DNA-RNA

ABSTRACT

Infection caused by Severe Acute Respiratory Syndrome Coronavirus-2 (SARS-CoV-2) is responsible for the Coronavirus disease (COVID-19) and the current pandemic. Its mortality rate increases, demonstrating the imperative need for acute and rapid diagnostic tools as an alternative to current serological tests and molecular techniques. Features of electrochemical genosensor devices make them amenable for fast and accurate testing closer to the patient. This work reports on a specific electrochemical genosensor for SARS-CoV-2 detection and discrimination against homologous respiratory viruses. The electrochemical biosensor was assembled by immobilizing thiolated capture probes on top of maleimide-coated magnetic particles, followed by specific target hybridization between the capture and biotinylated signaling probes in a sandwich-type manner. The probes were rigorously designed bioinformatically and tested in vitro. Enzymatic complexes based on streptavidin-horseradish peroxidase linked the biotinylated signaling probe to render the biosensor electrochemical response. The genosensor showed to reach a sensitivity of 174.4 μA fM^{-1} and a limit of detection of 807 fM when using streptavidin poly-HRP20 enzymatic complex, detected SARS-CoV-2 specifically and discriminated it against homologous viruses in spiked samples and samples from SARS-CoV-2 cell cultures, a step forward to detect SARS-CoV-2 closer to the patient as a promising way for diagnosis and surveillance of COVID-19.

1. Introduction

Human coronaviruses (HCoVs) were discovered in the 1960s, and since then, more HCoVs have been reported, including SARS-CoV, and Middle East Respiratory Syndrome (MERS), with a high potential to induce fatal respiratory disease in humans [1]. Unlike alfa-coronavirus such as HCoVOC43, HCo229E, HCoNL63, and Human Coronavirus (HKU1) that have been shown to cause common cold symptoms in immunocompetent humans, SARS-CoV and MERS-CoV induce severe respiratory failure [2] and high mortality rate [3]. At the end of 2019, a novel Coronavirus (SARS-CoV-2) spread rapidly worldwide, generating a public health problem [4,5]. This single-stranded RNA virus is responsible for COVID-19 and the current COVID-19 pandemic [6,7]. SARS-CoV-2 is transmitted from human to human through virus-containing droplets expulsed from an infected individual by coughing, sneezing, speaking, and breathing [8]. COVID-19 infection causes respiratory, gastrointestinal, liver, and neurological failures in symptomatic patients, among other symptoms depending on each person's health status [9].

The current clinical diagnosis of the SARS-CoV-2 is mainly based on detecting the viral RNA material through reverse transcriptase real-time Polymerase Chain Reaction (RT real-time PCR) [10,11]. The detection of COVID-19 also deals with antigen detection by lateral flow-based assays [12] or serological tests that employ antibodies to detect immunoglobulins that result from the inflammation process caused by the SARS-CoV-2 infection [11,13]. Other methods include aptamer- and CRISPR-based approaches, among many others [11,13]. Molecular techniques are considered the "gold standard" for SARS-CoV-2 detection and other pathologies involving DNA (RNA) sequence detection. Although RT-PCR is highly efficient, some drawbacks stem from the need for well-trained personnel, expensive instrumentation, time-consuming sample preparation and analysis, and lack of massive availability in all world regions [14,15]; and serological tests may suffer from cross-reactivity. In this context and because of the fast-spreading of new variants of the SARS-CoV-2, developing a simple, fast, accurate, easy-to-use, and sensitive detection tool is still an imperative need.

Biosensors have the potential to circumvent limitations of the current clinical assays in terms of portability and easiness to use near to the patient [16], being ideal devices for point-of-care (POC) or bedside testing [15–17]. Some researchers have reported electrochemical

* Corresponding author.
E-mail address: grupotandem.nanobioe@udea.edu.co (J. Orozco).

https://doi.org/10.1016/j.talanta.2022.123482
Received 15 February 2022; Received in revised form 8 April 2022; Accepted 13 April 2022
Available online 16 April 2022

biosensors to detect specific DNA/RNA sequences associated with viral infections [18,19], toxic species [20,21], and cancer biomarkers [22,23], among other pathologies [24] at low concentrations levels. However, only a few reports have detected SARS-CoV-2 with electrochemical biosensors [25,26], albeit no one is based on the format explored herein. For instance, an ultrasensitive electrochemical biosensor was assembled with magnetic particles decorated with gold nanoparticles and functionalized with a capture DNA probe to detect the virus in a sandwich-like format with a smartphone readout [27]. The S and N genes were detected based on isothermal rolling circle amplification with magnetic nanoparticles as sensing platform [28] and the N gene on a glassy carbon electrode functionalized with polymerized polyaniline nanowires [29]. Gold microelectrode array microchips have been combined with isothermal amplification to detect RNA-dependent polymerase and N genes [30]. Catalytic hairpin assembly with ruthenium complex was reported as a signal amplification strategy [31]. Other few authors have also reported electrochemical biosensors for N gene detection [32] for the detection of spike protein [33–40], immunoglobulins IgG and IgM [15], and pseudotyped viral particles [41,42]. An immunosensor [43] and a peptide-based biosensor [44] were recently reported by our group to rapidly detect the spike protein and the viral particles in clinical samples with simple electrochemical formats and values correlated with the RT-PCR standard method.

This work reports on an electrochemical biosensor for the specific detection of SARS-CoV-2 and discrimination against SARS-CoV, MERS, and HKU1 homologous viruses. All SARS-CoV-2 genomes reported in the databases were screened by a step-by-step rigorous bioinformatic protocol to select the conserved target regions [17] and design some forward and reverse primers, whose amplification capacity and specificity were verified in vitro. Capture and signaling probes were also designed from the target sequences for the biosensor construction. The biosensor was assembled on maleimide-modified magnetic beads (MMB) by binding thiolated capture probes that hybridized first the target and later the biotinylated signaling probe in a sandwich-type format. The biotinylated signaling probe allows the interaction with one of three different protein-enzyme complexes that contain a different number of HRP molecules to produce the final biosensor response by chronoamperometry. The electrochemical genosensor demonstrated the ability to discriminate SARS-CoV-2 when tested against SARS-CoV, MERS, and HKU1 homologous viruses and detected the genetic material in samples coming from SARS-CoV-2 cell cultures. The proposed biosystem holds the potential to detect genetic material in infected patients and asymptomatic individuals and is a step forward in developing highly sensitive genosensors to fight against the COVID-19 pandemic.

2. Materials and methods

The supporting information (S·I) section contains all reagents, SARS-CoV-2 probes, solutions, and equipment for the biosensing platform's development and characterization. The activation process of screen-printed gold electrodes (SPAuE) for biosensor development was carried out based on our previous works [17,18]. Bioinformatic design of the specific SARS-CoV-2 probes, screening procedure of the main parameters involved in the genosensing platform, and denaturation of RNA genetic material from cell culture are summarized in the S·I and in the sections below.

2.1. Bioinformatic design

An exhaustive search of all sequences deposited in the Genbank database from the National Center for Biotechnology Information (NCBI) was achieved first. The SARS-CoV-2 whole-genome sequences were screened from the beginning of the pandemic until April the 24th, 2020, resulting in 1112 conserved genomes selected and downloaded in fasta format. The downloaded genomic sequences were compiled as a "multifasta" file and aligned by the bioinformatic server Clustal Omega/Multiple Sequence Alignment. Jalview and Bioedit software allowed us to align and choose the most conserved regions of SARS-CoV-2 genomes, all coming from *Homo Sapiens Sapiens samples* [17].

2.2. Optimization of the genosensing platform

The main parameters involved in the biosensor assembly, such as the number of particles, enzyme complex-, target-, and signaling probe-concentrations, were optimized. The biosensing platform was built by linking a sulphydryl-reactive capture probe onto maleimide-functionalized magnetic beads. In a sandwich-like format, the modified particles hybridized the target probe with a biotinylated signaling probe. An enzymatic complex acting as a labeling tag was then anchored to the signaling probe to complete the biosensing platform. A commercial TMB solution containing 10 mM H_2O_2 was then added and the system was kept stirring at 800 rpm and room temperature for 20 min. The reaction solution produced a color change measured on a Thermo Scientific Microplate Spectrophotometer (VARIOSKAN LUX) at a wavelength of 620 nm that was target concentration-dependent, serving as a rapid screening method of all variables mentioned. In the electrochemical genosensors, the response came from the TMB reduction by applying a constant voltage of −150 mV for 60 s in a potentiostat PalmSens3 with software PSTrace version 5.8. The synthetic DNA strands of SARS-CoV-2 (strain from Wuhan) and the same sequence with one and two mismatches were evaluated, and those from its SARS-CoV, MERS and HKU1 homologous are described in Table 1.

2.3. Detection of genetic material in cell culture samples

We first evaluated the specificity of the biosensor by testing one and two base mismatches (mismatch 1 and mismatch 2) from the H conserved region of SARS-CoV-2 against SARS-CoV, MERS, and HKU1 counterparts at three different target concentrations (see Table 1). Similarly, by employing the same procedure for synthetic DNA, we challenged the genosensing platform with a real RNA sample from a cell culture with a total RNA/DNA load of 36.8 ng/mL (1.89 pM).

2.4. Statistical analysis

Numerical data were expressed as the mean ± standard deviation (SD) and compared statistically using Student's t-test or one-way ANOVA followed by the Bonferroni test, with $p < 0.05$ indicating significance and the GraphPad Prism 5.01 version for Windows (GraphPad Software, San Diego, CA, USA, 2007).

3. Results and discussion

Genosensors are devices based on nucleotide sequences that act as bioreceptors for the specific biorecognition of complementary DNA/RNA target probes. The biorecognition event is commonly achieved in a sandwich-type assembly by the Watson and Crick complementarity between nitrogenous bases from bioreceptors and target sequences in hybridization conditions. The genosensor was assembled on top of MMB by linking a thiol-labeled capture probe by a covalent bound [45]. Then, the viral RNA target sequence was hybridized between the thiolated capture probe and a biotinylated signaling probe. Three different protein-enzyme complexes -i.e., streptavidin-HRP, streptavidin poly-HRP20 or streptavidin poly-HRP80, containing a different quantity of HRP molecules were specifically bonded with biotin from the signaling probe to complete the biosensing platform. Finally, the biosensor performance was interrogated with TMB, an HRP enzyme-substrate, by following its oxidized colored product in the presence of hydrogen peroxide. The color change followed by spectrophotometry rapidly screened all the genosensor assembly variables detailed in the experimental section. Besides, the oxidized product was electrochemically reduced by transferring the magnetic bead-based

Table 1
DNA probes designed for the specific detection of SARS-CoV-2.

Probes		Sequences (5'->3')	5′	3′
Capture probe	**H**	TGCCTACAGTACTCAGAATCAAAAG	**-**	**SH**
	I	GGAAACACCATTAAAGACTACACGT	**-**	**SH**
	A	TCTGTAAAACACGCACAGAATTTTG	**-**	**SH**
Signaling probe	**H**	CTTCTGATCTTTCACAAGTGCCG	**Bio**	**-**
	I	CGCAGCTTCTTCAAAAGTACTAAA	**Bio**	**-**
	A	CCATCTAGTATTGTTATAGCGGCCT	**Bio**	**-**
Target probes				
SARS-CoV-2	**H**	CTTTTGATTCTGAGTACTGTAGGCACGGCACTTGTGAAAGATCAGAAG		
	I	ACGTGTAGTCTTTAATGGTGTTTCCTTTAGTACTTTTGAAGAAGCTGCG		
	A	CAAAATTCTGTGCGTGTTTTACAGAAGGCCGCTATAACAATACTAGATGG		
SARS-CoV		CTTTTGATGCTGAGTACTGTAGACATGGTACATGCGAAAGGTCAGAAG		
MERS		CTCTGTCAACTCAGTACTGCCGGTTCGGTAGTTGTGAGTATGCACAAG		
HKU1		CGCGCTCTATGACTTATTGTAGAGTGGGTGCATGTGAATACGCCGAAG		
MISMATCH-1		CTTTTGATT**A**TGAGTACTGTAGGCACGGCACTTGTGAAAGATCAGAAG		
MISMATCH-2		CTTTTGATT**A**TGAGTACTGTAGGC**C**CGGCACTTGTGAAAGATCAGAAG		

Bio, Biotynilated probe; SH, Thiolated probe.

biosensor assembly to the surface of an SPAuE and recording the current signal resulting from the TMB-electrode charge transfer after applying a cathodic potential, which was DNA(RNA) concentration-dependant.

3.1. Bioinformatic design

After downloading and aligning the SARS-CoV-2 genome sequences, excluding gaps and sequence incompatibilities, 1104 genomic sequences were employed to search for the conserved regions. The first screening was based on having at least 70 nucleotides in length as minimal sequence extension, where 52 conserved sequences were identified and screened by *Blast nucleotide* to find the conserved sequences that do not match with previously reported coronaviruses. Next, the selected SARS-CoV-2 conserved regions' homology was interrogated against alfa-coronavirus HCoV-NL63, HCoV229E, HCoVOC43, HCoVHKU, MERS, and SARS-CoV, and the human genome, demonstrating not to present homology among all tested genomes. Finally, we selected three phylogenetically conserved regions with an appropriate length range from 18 to 25 nucleotides and fulfilled all thermodynamic requirements [17]. We designed 3′end thiolated capture probes and 5′end biotinylated signaling probes for each target's genosensor assembly as a template. Table 1 summarizes the selected conserved target regions, the designed capture and signaling probes, the sequences of homologous SARS-CoV-2, and one and two base pair mismatches concerning the SARS-CoV-2 H-conserved sequence.

3.2. Optimization of the genosensing platform

The following experiments describe optimizing the main variables involved in the electrochemical genosensor assembly rapidly screened by spectrophotometry. First, the quantity of MMB, enzyme, capture, and signaling probes concentration were optimized with a fixed concentration of the H-conserved target region of the SARS-CoV-2 of 0.1 μM (see the sequence in Table 1). Next, the concentration of MMB was interrogated from 0 to 30 μg. Fig. 1A shows that the biosensor reached a plateau after 10 μg of MMB, indicating the saturation of colorimetric signal response. The particle concentration higher than 10 μg did not show any signal improvement; hence 10 μg of MMB was established as the optimal

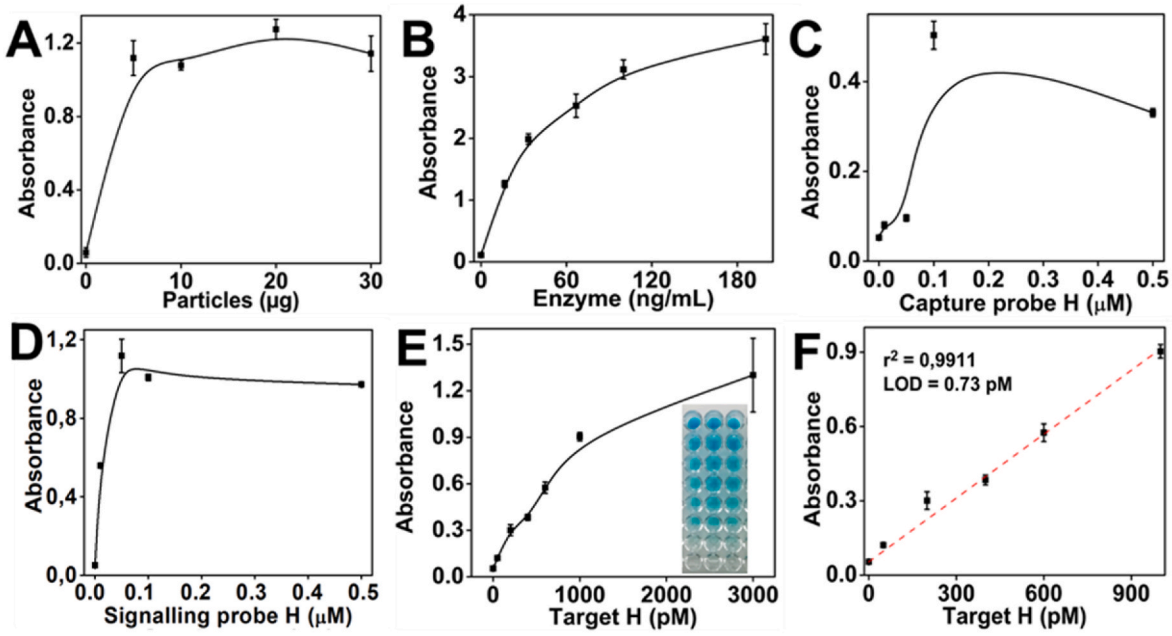

Fig. 1. Screening the main parameters involved in developing a genosensing platform by spectrophotometry **A)** particle **B)** enzyme **C)** capture probe **D)** signaling probe concentrations for the H-conserved region of SARS-CoV-2, **E)** Resulting colorimetric calibration curve (original wells are in the inset) and **F)** the corresponding linear region. Error bars indicate the standard deviation of triplicate measurements.

particle amount for further optimizations. The streptavidin poly-HRP enzymatic complex's concentration, responsible for the signal biosensor response, was tested in concentrations from 0 to 200 ng/mL. The results indicate that the colorimetric response of the biosensor increased as the enzyme did. Nevertheless, concentrations higher than 16.6 ng/mL did not follow the Beer-Lambert law [46], being such concentration selected as optimal (see Fig. 1B). Finally, concentrations of the thiolated capture probe coupled to the MMB surface and the biotinylated signaling probe linked to the streptavidin poly-HRP complex were tested from 0 to 0.5 μM. Fig. 1C and D show the signal response reached a plateau with concentrations of capture and signaling probes equal to or higher than 0.1 μM, respectively, selected as the optimal concentrations. Interestingly, higher concentrations in both cases did not show any signal enhancement. As shown in Table 1, two additional pairs of capture and signaling probes (I and A) were designed similarly to those detailed in the previous section to bind to I and A conserved regions of SARS-CoV-2, respectively. The capture and signaling probes were tested in the same concentration range as per target H, as shown in Fig. S1A and S1B, with identical results. It indicates that optimal capture and signaling probes are similar for all conserved regions and that the system is highly reproducible. Table 2 summarizes the optimized parameters in the biosensor development screened by colorimetric measurements.

After optimizing the genosensing assembly, it was challenged with different target concentrations of SARS-CoV-2 sequences, employing two different enzymatic streptavidin-HRP conjugates. Fig. 1E shows the resulting colorimetric calibration curve in an H-conserved SARS-CoV-2 target-dependent manner from 0 to 3000 pM and Fig. 1F shows the corresponding linear region. The results indicate a linear behavior ranging from 0 to 1000 pM when using streptavidin-HRP as a signaling tag. Similarly, other calibration curves with I- and A-conserved regions of SARS-CoV-2 using streptavidin-HRP are shown in Fig. S2A and S2B and the corresponding linear regions in S2C and S2D, respectively. Based on the colorimetric biosensor working range and the achieved limit of detection (LOD), the H-conserved region of the SARS-CoV-2 virus was chosen as the optimal DNA sequence to perform the following set of experiments. The selected H-conserved region was also tested with the streptavidin-poly-HRP20 enzymatic complex to improve the biosensor performance. Such conjugate contains 100 HRP molecules per streptavidin molecule, which is expected to amplify the signal response dramatically. Fig. S3A shows the colorimetric response by testing different target concentrations ranging from 0 to 600 pM and Fig. S3B shows the corresponding linear region. Table 2 summarizes the analytical parameters for the screening colorimetric assays. Results demonstrate that the sensitivity of the H-conserved region genosensor with streptavidin-poly-HRP20 increased 15-fold concerning its streptavidin-HRP counterpart. The complex also demonstrated to lower the LOD 12-fold notwithstanding a narrower working range.

Towards developing a portable, easy-to-use genosensor with minimal consumption of reagents and samples and a direct sample readout closer to the patient, we moved to an electrochemical format. The MMB-based genonsensing assembly was confined onto the surface of the SPAuE by a magnet to test its performance in a portable and easy-to-use electrochemical workstation. Optimal enzyme, capture, and signaling probe concentrations were verified with the H-conserved region of SARS-CoV-2 genetic material by chronoamperometry. Noticeably, the enzyme complex was optimized based on the signal/noise (S/N) ratio, and several washing steps were implemented during particle sensitization and before the final measurements to prevent non-specific interactions that may induce a high signal background. A set of streptavidin-HRP conjugates, including streptavidin-HRP, streptavidin poly-HRP20, and streptavidin poly-HRP80, containing 1, 100, and 400 molecules of HRP per each streptavidin molecule, respectively, were compared to select the one of higher signal amplification capability [47]. Fig. 2A, S3A, and S3B show results from the three different enzymatic complexes tested with 0–100 ng/mL, including a negative control with water instead of viral genetic material. Based on the S/N ratio, the optimal enzyme concentration was 66.7 ng/mL for all cases because of the lower standard deviation of the resultant signals, and it spends a reasonable amount of this reagent while still having a high enough positive signal with low background. Yet, based on the three enzymatic complexes studied, streptavidin-HRP showed the lowest signal amplification response at the optimal enzyme concentration of 66.7 ng/mL. In contrast, streptavidin poly-HRP20 and streptavidin poly-HRP80 reached a similar maximum current value, but streptavidin poly-HRP20 had a lower background. The capture and signaling probes concentration were double-checked from 0 to 0.5 μM. It was confirmed that 0.1 μM streptavidin poly-HRP20 was the optimal enzyme complex and concentration in both cases as a signaling tag (Fig. 2B and C) concerning the streptavidin-HRP and streptavidin poly-HRP80 counterparts. Fig. S4A- and S4B show optimization of the capture probe and signaling probes with streptavidin-HRP and streptavidin poly-HRP80, respectively. The results showed a good correlation between spectrophotometry and chronoamperometry measurements, indicating that the genosensor assembly's signal response could be followed by either method on a laboratory bench or closer to the patient, respectively. The optimized parameters in the electrochemical biosensing platform are summarized in Table 3.

Once all electrochemical parameters were optimized, the device's analytical performance was tested. Fig. 3A–C (upper part) show the chronoamperometric current profiles depending on the target concentration for the three employed enzymatic conjugates streptavidin-HRP, streptavidin poly-HRP20, and streptavidin poly-HRP80, respectively, and the corresponding linear ranges in Fig. 3A–C (bottom part). Chronoamperometric measurements at high target concentrations seem to show limitations of the electrochemical probe diffusion process related to enzyme complex accumulation at the magnetic beads. Yet, as interpolation of current intensity was after 60 s, the stationary state was ensured, and the reproducibility and reliability of the results were guaranteed. The electrochemical biosensor exhibited a broader linear range using streptavidin-HRP to amplify the signal than the other enzymatic complexes studied. However, streptavidin poly-HRP20 and streptavidin-poly-HRP80 exhibited improved sensitivity and LOD concerning streptavidin-HRP. For example, the sensitivity of the genosensor amplified with streptavidin poly-HRP20 and streptavidin poly-HRP80 was ~62- and 91-fold higher than that of streptavidin-HRP. Consequently, the LODs went down ~75- and 100-fold, respectively. It demonstrated streptavidin poly-HRP20 and streptavidin poly-HRP80 comparable performance but better than streptavidin-HRP.

The higher HRP molecules of streptavidin poly-HRP80 concerning the streptavidin poly-HRP20 enzymatic complex expect the highest electrochemical biosensing signal response [44]; however, the biosensing response was quite comparable in both cases. We hypothesized that having a complex with a higher number of molecules as a signaling tag may induce steric repulsion, limiting the contact of streptavidin poly-HRP80 complex with the biotinylated signaling probes, leading to a slightly reduced biosensing response to streptavidin-HRP20. Besides,

Table 2
Analytic performance of the genosensor screened by spectrophotometry.

Parameter	Range		Optimal
Particles (μg)	0–30		10
Enzyme concentration (ng/mL)	0–200		16.6
Capture probe region A, H, I (μM)	0–0.5		0.1
Signaling probe region A, H, I (μM)	0–0.5		0.1
Analytical performance			
Region	**Range (pM)**	**LOD (pM)**	**Sensitivity (fM^{-1})**	**r^2**
I	0–6000	94	0.2	0.9933
A	0–800	0.75	1.6	0.9974
H	0–1000	0.73	0.8	0.9911
H poly-HRP-20	0–100	0.06	12	0.9933

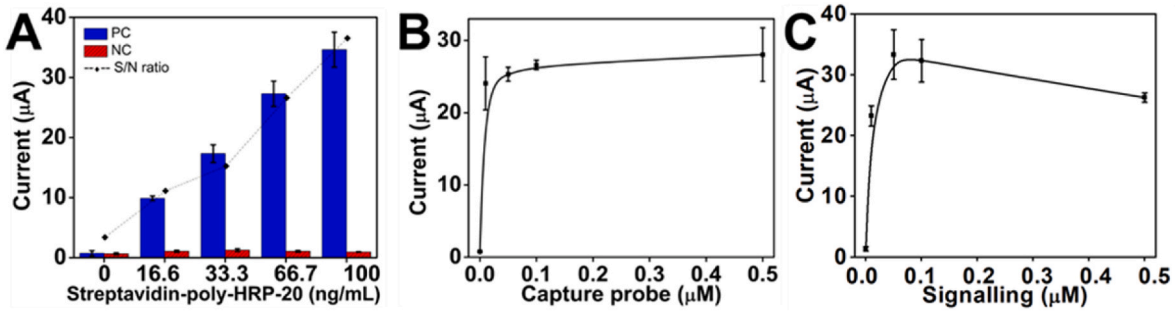

Fig. 2. Optimization of parameters involved in the electrochemical genosensor assembly **A) s**treptavidin poly-HRP20 enzymatic complex, **B)** capture and **C)** signaling probe concentrations for the H-conserved region SARS-CoV-2. Error bars indicate the standard deviation of triplicate measurements. In panel 2A, PC, Positive control; NC, Negative control; S/N, signal to noise ratio.

Table 3
Analytical performance of the electrochemical genosensors.

Parameter			Range	Optimal
Enzyme concentration (ng/ml) Strep-HRP, strep-poly-HRP20, strep-poly-HRP80			0–100	66.7
Capture probe (μM) Strep-HRP, strep-poly-HRP20, strep-poly-HRP80			0–0.5	0.1
Signaling probe (μM) Strep-HRP, strep-poly-HRP20, strep-poly-HRP80			0–0.5	0.1
Analytical performance **Region (signal amplification)**	**Range (pM)**	**LOD (pM)**	**Sensitivity (μA fM^{-1})**	**r^2**
H (HRP)	0–800	60	2.8	0.9921
H (poly-HRP-20)	0–80	0.8	174.4	0.9981
H (poly-HRP-80)	0–100	0.6	255.9	0.9936

non-specific interactions of enzymatic complexes with higher HRP molecules may produce higher backgrounds [47] (see Fig. 2A and S4B). Literature reports support well-distributed capture probes significantly influence the final biosensing response [47–49]. Such biosensors showed tetrahedral capture DNA probes to improve the capture probe distribution on the biosensor's surface. The tetrahedral DNA nanostructure reduced steric repulsion and helped minimize the background due to its capacity to act as a resistant protein [47,50]. For the above, we choose streptavidin poly-HRP20 as the optimal enzymatic complex for the electrochemical genosensor despite the slightly lower signal response, but it reached the lowest background. Table 3 summarizes the analytical characteristics of the genosensing devices.

3.3. Specificity and detection of genetic material in samples

The feasibility of the as-developed electrochemical genosensing platform to specifically detect the SARS-CoV-2 was interrogated. For this purpose, the electrochemical biosensing platform's potential to discriminate one and two mismatches in DNA synthetic sequences from SARS-CoV-2 and sequences from other related coronaviruses was evaluated. The electrochemical platform was tested against one and two base pair mismatches from the H-conserved region of SARS-CoV-2 and SARS-CoV, MERS, and HKU1 homologous counterparts, with three loads of target DNA sequences of 10, 100 and 1000 pM and compared with negative controls (NC) which consisted of only a buffer solution. Fig. 4A shows that the current response of the genosensor for the SARS-CoV-2 DNA sequence was dramatically higher than that of the NC, the one and two base pair mismatches, and the other coronaviruses with three

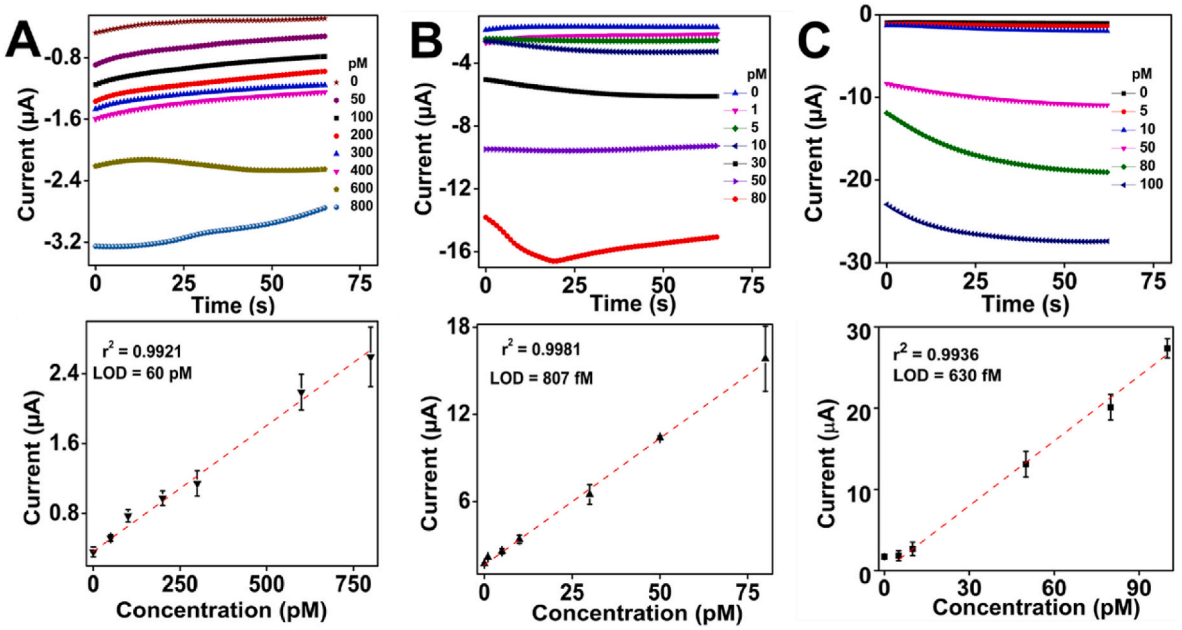

Fig. 3. Electrochemical response of the assembled genosensing platforms. Current profiles in a target-concentration-dependent manner for the H-conserved region of SARS-CoV-2 using different enzyme complexes, **A)** streptavidin-HRP, **B)** streptavidin poly-HRP20 and **C)** streptavidin poly-HRP80. Error bars indicate the standard deviation of triplicate measurements.

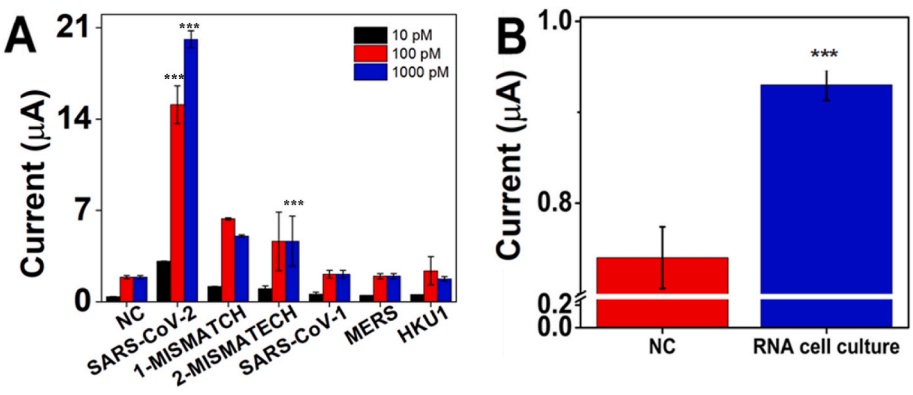

Fig. 4. Electrochemical genosensor response. **A)** Specificity evaluation against one and two base pair mismatches from H-conserved sequences of SARS-CoV-2 (mismatch 1 and mismatch 2) and SARS-CoV, MERS y HKU1 homologous counterparts at three different loads from 10 to 1000 pM. **B)** Genosensor response against a positive SARS-CoV-2 RNA cell culture sample compared with negative control (NC). The columns and points are the mean ± SD n = 3. *** represent statistical differences concerning negative control with a *p*-value < 0.05.

loads. A paired *t*-test and a 1-way ANOVA showed statistically significant differences, *p*-value < 0.05. Furthermore, the signal intensity of the genosensors with one and two mismatches was slightly higher than those from the other coronavirus, which indicates a low interaction between capture and signaling probes and the mismatched target sequences. However, the electrochemical biosensor could not detect SARS-CoV-2 homologous viruses even at a high concentration level (1000 pM), showing a current signal comparable to the NC with no statistically significant differences but statistically significant differences concerning the SARS-CoV-2 positive control, *p*-value < 0.05. Hence, the results reveal that the as-developed electrochemical biosensing platform is specific for detecting target sequences coming only from SARS-CoV-2 and can discriminate mismatched sequences and homologous viruses.

After specificity evaluation, we further interrogated the potential of the as-developed electrochemical genosensor to detect the SARS-CoV-2 in conditions closer to a real scenario by studying its performance in a sample coming from the virus-cell culture, having a total DNA/RNA viral load of 36.8 ng/mL (1.89 pM). Fig. 4B shows the electrochemical platform evaluation results with the cell culture sample and compares them to their corresponding NC. The results show differential biosensor response between the SARS-CoV-2 cell culture sample and the NC, with statistically significant differences, *p*-value < 0.05. Although this is the first approximation forward to a real scenario, the proof-of-concept demonstrated the potential of the electrochemical genosensor as a tool for virus detection. However, here it is essential to highlight that the electrochemical signal for the positive sample extracted from cell culture had a lower electrochemical response because the genetic material (1.89 pM total RNA/DNA) is lower than the synthetic DNA concentration tested (10, 100 and 1000 pM). Besides, while synthetic DNA samples correspond to a short ssDNA sequence, real samples correspond to the whole genome of SARS-CoV-2 fragmented randomly after the denaturalization protocol, generating small DNA/RNA fragments where not all correspond to specific fragments to hybridize with the capture and signaling probes. The as-developed biosensor is a promising approximation to the clinical diagnosis where the samples do not require either arduous sample preparation or amplification steps. Further work is directed to a complete validation procedure for the proposed electrochemical genosensor, analyzing a statistical number of positive and negative samples to evaluate the device's real potential as an analytical tool for detecting the SARS-CoV-2. Besides, coupling the biosensor to a loop-mediated isothermal amplification (LAMP) system is worth exploring.

4. Conclusions

We reported an electrochemical genosensor for the specific detection of SARS-CoV-2 and discrimination against SARS-CoV, MERS, and HKU1 homologs viruses. After an exhaustive and rigorous bioinformatic analysis, we designed three pairs of thiolated capture and biotinylated signaling probes for the SARS-CoV-2 electrochemical genosensor development. We assembled the genosensor, tested the proper probe design and optimized all other parameters needed. We tested the analytical performance of the resultant electrochemical genosensor by using three different enzymatic complexes, streptavidin-HRP streptavidin poly-HRP20, and streptavidin poly-HRP80. Enzymatic complexes containing more than one HRP molecule per streptavidin molecule were demonstrated to decrease the LOD from the pM to fM level. However, streptavidin-poly-HRP20 was the optimal signaling tag for the electrochemical genosensor assembly with a lowered current background. Furthermore, we demonstrated the electrochemical genosensor discriminated SARS-CoV2 against one and two base pairs mismatch from H-conserved region, SARS-CoV, MERS, and HKU1 sequences. Finally, the device detected RNA SARS-CoV-2 from cell culture concerning a negative control without genetic material. Overall, the results demonstrated that the genosensor platform could be an easy-to-use SARS-CoV-2 diagnostic tool with great potential to help in fighting the current pandemics.

Credit author statement

Sebastian Cajigas: Methodology, Writing – original draft, Investigation, Data curation, Formal analysis. Daniel Alzate: Methodology, Investigation, Data curation, Formal analysis. Maritza Fernández: Formal analysis, Review & Editing. Carlos Muskus: Conceptualization, Formal analysis, Funding acquisition. Jahir Orozco: Funding acquisition, Conceptualization, Formal analysis, Project administration, Supervision, Writing – original draft, Review and Editing. All authors read and agreed with the manuscript.

Declaration of competing interest

The authors declare that they have no known competing financial interests or personal relationships that could have appeared to influence the work reported in this paper.

Acknowledgments

This work has been funded by Ministerio de ciencia y tecnología MINCIENCIAS (Mincienciatón, project number 1115101576765). J. O acknowledges financial support from the Minciencias, the University of Antioquia and the Max Planck Society through the Cooperation agreement 566-1, 2014. Furthermore, we thank The Ruta N complex for hosting the Max Planck Tandem Groups.

Appendix A. Supplementary data

Supplementary data to this article can be found online at https://doi.org/10.1016/j.talanta.2022.123482.

References

[1] S. Su, G. Wong, W. Shi, J. Liu, A.C.K. Lai, J. Zhou, W. Liu, Y. Bi, G.F. Gao, Epidemiology, genetic recombination, and pathogenesis of coronaviruses, Trends Microbiol. 24 (2016) 490–502, https://doi.org/10.1016/j.tim.2016.03.003.

[2] P. Moitra, M. Alafeef, M. Alafeef, M. Alafeef, K. Dighe, M.B. Frieman, D. Pan, D. Pan, D. Pan, Selective naked-eye detection of SARS-CoV-2 mediated by N gene targeted antisense oligonucleotide capped plasmonic nanoparticles, ACS Nano 14 (2020) 7617–7627, https://doi.org/10.1021/acsnano.0c03822.

[3] X. Yuan, C. Yang, Q. He, J. Chen, D. Yu, J. Li, S. Zhai, Z. Qin, K. Du, Z. Chu, P. Qin, Current and perspective diagnostic techniques for COVID-19, ACS Infect. Dis. 6 (2020), https://doi.org/10.1021/acsinfecdis.0c00365, 1998–2016.

[4] K.G. Andersen, A. Rambaut, W.I. Lipkin, E.C. Holmes, R.F. Garry, The proximal origin of SARS-CoV-2, Nat. Med. 26 (2020) 450–452.

[5] F. Cui, H.S. Zhou, Diagnostic methods and potential portable biosensors for coronavirus disease 2019, Biosens. Bioelectron. 165 (2020) 112349, https://doi.org/10.1016/j.bios.2020.112349.

[6] W.E. Wei, Z. Li, C.J. Chiew, S.E. Yong, M.P. Toh, V.J. Lee, Presymptomatic transmission of SARS-CoV-2—Singapore, january 23–march 16, 2020, Morb. Mortal. Wkly. Rep. 69 (2020) 411.

[7] B. Hu, H. Guo, P. Zhou, Z.-L. Shi, Characteristics of SARS-CoV-2 and COVID-19, Nat. Rev. Microbiol. (2020) 1–14.

[8] B.K.A. Prather, C.C. Wang, R.T. Schooley, Reducing transmission of SARS-CoV-2, Science 368 (2020) 1422–1424.

[9] D. Wu, T. Wu, Q. Liu, Z. Yang, The SARS-CoV-2 outbreak: what we know, Int. J. Infect. Dis. 94 (2020) 44–48, https://doi.org/10.1016/j.ijid.2020.03.004.

[10] K.A. Walsh, K. Jordan, B. Clyne, D. Rohde, L. Drummond, P. Byrne, S. Ahern, P. G. Carty, K.K. O'Brien, E. O'Murchu, SARS-CoV-2 detection, viral load and infectivity over the course of an infection, J. Infect. 81 (2020) 357–371.

[11] R. Jalandra, A.K. Yadav, D. Verma, N. Dalal, M. Sharma, R. Singh, A. Kumar, P. R. Solanki, Strategies and perspectives to develop SARS-CoV-2 detection methods and diagnostics, Biomed. Pharmacother. (2020) 110446.

[12] M. Yüce, E. Filiztekin, K.G. Özkaya, COVID-19 diagnosis —a review of current methods, Biosens. Bioelectron. 172 (2021), https://doi.org/10.1016/j.bios.2020.112752.

[13] M.L. Bastos, G. Tavaziva, S.K. Abidi, J.R. Campbell, L.-P. Haraoui, J.C. Johnston, Z. Lan, S. Law, E. MacLean, A. Trajman, Diagnostic accuracy of serological tests for covid-19: systematic review and meta-analysis, BMJ 370 (2020).

[14] R. Wang, C. Qian, Y. Pang, M. Li, Y. Yang, H. Ma, M. Zhao, F. Qian, H. Yu, Z. Liu, opvCRISPR: one-pot visual RT-LAMP-CRISPR platform for SARS-cov-2 detection, Biosens. Bioelectron. 172 (2021) 112766.

[15] A. Yakoh, U. Pimpitak, S. Rengpipat, N. Hirankarn, O. Chailapakul, S. Chaiyo, Paper-based electrochemical biosensor for diagnosing COVID-19: detection of SARS-CoV-2 antibodies and antigen, Biosens, Bioelectron 176 (2021) 112912, https://doi.org/10.1016/j.bios.2020.112912.

[16] T. Nguyen, V.A. Chidambara, S.Z. Andreasen, M. Golabi, V.N. Huynh, Q.T. Linh, D. D. Bang, A. Wolff, Point-of-care devices for pathogen detections: the three most important factors to realise towards commercialization, TrAC Trends Anal. Chem. (Reference Ed.) 131 (2020) 116004, https://doi.org/10.1016/j.trac.2020.116004.

[17] J. Kudr, P. Michalek, L. Ilieva, V. Adam, O. Zitka, COVID-19: a challenge for electrochemical biosensors, TrAC Trends Anal. Chem. (Reference Ed.) 136 (2021) 116192, https://doi.org/10.1016/j.trac.2021.116192.

[18] D. Alzate, S. Cajigas, S. Robledo, C. Muskus, J. Orozco, Genosensor for differential detection of Zika virus, Talanta 210 (2020) 120648.

[19] S. Cajigas, D. Alzate, J. Orozco, Gold nanoparticle/DNA-based nanobioconjugate for electrochemical detection of Zika virus, Microchim. Acta 187 (2020), https://doi.org/10.1007/s00604-020-04568-1.

[20] J. Orozco, E. Villa, C.L. Manes, L.K. Medlin, D. Guillebault, Electrochemical RNA genosensors for toxic algal species: enhancing selectivity and sensitivity, Talanta 161 (2016) 560–566.

[21] J. Orozco, L.K. Medlin, Electrochemical performance of a DNA-based sensor device for detecting toxic algae, Sensor. Actuator. B Chem. 153 (2011) 71–77.

[22] S. Su, W. Cao, W. Liu, Z. Lu, D. Zhu, J. Chao, L. Weng, L. Wang, C. Fan, L. Wang, Dual-mode electrochemical analysis of microRNA-21 using gold nanoparticle-decorated MoS2 nanosheet, Biosens. Bioelectron. 94 (2017) 552–559, https://doi.org/10.1016/j.bios.2017.03.040.

[23] D. Zhu, W. Liu, W. Cao, J. Chao, S. Su, L. Wang, C. Fan, Multiple amplified electrochemical detection of MicroRNA-21 using hierarchical flower-like gold nanostructures combined with gold-enriched hybridization Chain reaction, Electroanalysis 30 (2018) 1349–1356.

[24] S. Han, W. Liu, M. Zheng, R. Wang, Label-Free and ultrasensitive electrochemical DNA biosensor based on urchinlike carbon nanotube-gold nanoparticle nanoclusters, Anal. Chem. 92 (2020) 4780–4787.

[25] N. Bhalla, Y. Pan, Z. Yang, A.F. Payam, Opportunities and challenges for biosensors and nanoscale Analytical tools for pandemics: COVID-19, ACS Nano 14 (2020) 7783–7807, https://doi.org/10.1021/acsnano.0c04421.

[26] R.R.X. Lim, A. Bonanni, The potential of electrochemistry for the detection of coronavirus-induced infections, TrAC Trends Anal. Chem. (Reference Ed.) 133 (2020) 116081, https://doi.org/10.1016/j.trac.2020.116081.

[27] H. Zhao, F. Liu, W. Xie, T.C. Zhou, J. OuYang, L. Jin, H. Li, C.Y. Zhao, L. Zhang, J. Wei, Y.P. Zhang, C.P. Li, Ultrasensitive supersandwich-type electrochemical sensor for SARS-CoV-2 from the infected COVID-19 patients using a smartphone, Sensor. Actuator. B Chem. 327 (2021) 128899, https://doi.org/10.1016/j.snb.2020.128899.

[28] T. Chaibun, J. Puenpa, T. Ngamdee, N. Boonapatcharoen, P. Athamanolap, A. P. O'Mullane, S. Vongpunsawad, Y. Poovorawan, S.Y. Lee, B. Lertanantawong, Rapid electrochemical detection of coronavirus SARS-CoV-2, Nat. Commun. 12 (2021) 1–10, https://doi.org/10.1038/s41467-021-21121-7.

[29] Z. Song, Y. Ma, M. Chen, A. Ambrosi, C. Ding, X. Luo, Electrochemical biosensor with enhanced antifouling capability for COVID-19 nucleic acid detection in complex biological media, Anal. Chem. 93 (2021) 5963–5971, https://doi.org/10.1021/acs.analchem.1c00724.

[30] H.E. Kim, A. Schuck, S.H. Lee, Y. Lee, M. Kang, Y.S. Kim, Sensitive electrochemical biosensor combined with isothermal amplification for point-of-care COVID-19 tests, Biosens. Bioelectron. 182 (2021), https://doi.org/10.1016/j.bios.2021.113168.

[31] Y. Peng, Y. Pan, Z. Sun, J. Li, Y. Yi, J. Yang, G. Li, An electrochemical biosensor for sensitive analysis of the SARS-CoV-2 RNA, Biosens. Bioelectron. 186 (2021) 113309, https://doi.org/10.1016/j.bios.2021.113309.

[32] M. Alafeef, K. Dighe, P. Moitra, D. Pan, Rapid, ultrasensitive, and quantitative detection of SARS-CoV-2 using antisense oligonucleotides directed electrochemical biosensor chip, ACS Nano 14 (2020) 17028–17045.

[33] S. Mavrikou, G. Moschopoulou, V. Tsekouras, Development of a portable, ultra-rapid and ultra-sensitive cell-based biosensor for the direct detection of the SARS-CoV-2 S1 spike protein antigen, Sensors 20 (2020) 3121.

[34] V.J. Vezza, A. Butterworth, P. Lasserre, E.O. Blair, A. MacDonald, S. Hannah, C. Rinaldi, P.A. Hoskisson, A.C. Ward, A. Longmuir, S. Setford, E.C.W. Farmer, M. E. Murphy, D.K. Corrigan, An electrochemical SARS-CoV-2 biosensor inspired by glucose test strip manufacturing processes, Chem. Commun. 57 (2021) 3704–3707, https://doi.org/10.1039/d1cc00936b.

[35] Z. Rahmati, M. Roushani, H. Hosseini, H. Choobin, Electrochemical immunosensor with Cu2O nanocube coating for detection of SARS-CoV-2 spike protein, Microchim. Acta 188 (2021), https://doi.org/10.1007/s00604-021-04762-9.

[36] B. Mojsoska, S. Larsen, D.A. Olsen, J.S. Madsen, I. Brandslund, F.A. Alatraktchi, Rapid SARS-CoV-2 detection using electrochemical immunosensor, Sensors 21 (2021) 1–11, https://doi.org/10.3390/s21020390.

[37] B.S. Vadlamani, S.C. Verma, Functionalized TiO 2 nanotube-based electrochemical biosensor for rapid detection of SARS-CoV-2, Sensors 20 (2020) 1–10, https://doi.org/10.1101/2020.09.07.20190173.

[38] A. Raziq, A. Kidakova, R. Boroznjak, J. Reut, A. Öpik, V. Syritski, Development of a portable MIP-based electrochemical sensor for detection of SARS-CoV-2 antigen, Biosens. Bioelectron. 178 (2021), https://doi.org/10.1016/j.bios.2021.113029.

[39] J. Muñoz, M. Pumera, 3D-Printed COVID-19 immunosensors with electronic readout, Chem. Eng. J. 425 (2021), https://doi.org/10.1016/j.cej.2021.131433.

[40] A. Idili, C. Parolo, R. Alvarez-Diduk, A. Merkoçi, Rapid and efficient detection of the SARS-CoV-2 spike protein using an electrochemical aptamer-based sensor, ACS Sens. 6 (2021) 3093–3101, https://doi.org/10.1021/acssensors.1c01222.

[41] H. Yousefi, A. Mahmud, D. Chang, J. Das, S. Gomis, J.B. Chen, H. Wang, T. Been, L. Yip, E. Coomes, Z. Li, S. Mubareka, A. Mcgeer, N. Christie, S. Gray-Owen, A. Cochrane, J.M. Rini, E.H. Sargent, S.O. Kelley, Detection of SARS-CoV-2 viral particles using direct, reagent-free electrochemical sensing, J. Am. Chem. Soc. 143 (2021) 1722–1727, https://doi.org/10.1021/jacs.0c10810.

[42] S. Eissa, H.A. Alhadrami, M. Al-Mozaini, A.M. Hassan, M. Zourob, Voltammetric-based immunosensor for the detection of SARS-CoV-2 nucleocapsid antigen, Microchim. Acta 188 (2021), https://doi.org/10.1007/s00604-021-04867-1.

[43] V. Vásquez, M.-C. Navas, J.A. Jaimes, J. Orozco, SARS-CoV-2 electrochemical immunosensor based on the spike-ACE2 complex, Anal. Chim. Acta 1205 (2022) 339718, https://doi.org/10.1016/j.aca.2022.339718.

[44] D. Soto, J. Orozco, Peptide-based simple detection of SARS-CoV-2 with electrochemical readout, Anal. Chim. Acta 1205 (2022) 339739, https://doi.org/10.1016/j.aca.2022.339739.

[45] B.H. Northrop, S.H. Frayne, U. Choudhary, Thiol-maleimide "click" chemistry: evaluating the influence of solvent, initiator, and thiol on the reaction mechanism, kinetics, and selectivity, Polym. Chem. 6 (2015) 3415–3430, https://doi.org/10.1039/c5py00168d.

[46] D.F. Swinehart, The Beer-Lambert law, J. Chem. Educ. 39 (1962) 333–335, https://doi.org/10.1021/ed039p333.

[47] Y. Wen, L. Wang, L. Xu, L. Li, S. Ren, C. Cao, N. Jia, A. Aldalbahi, S. Song, J. Shi, J. Xia, G. Liu, X. Zuo, Electrochemical detection of PCR amplicons of: Escherichia coli genome based on DNA nanostructural probes and polyHRP enzyme, Analyst 141 (2016) 5304–5310, https://doi.org/10.1039/c6an01435f.

[48] D. Chen, D. Wang, X. Hu, G. Long, Y. Zhang, L. Zhou, A DNA nanostructured biosensor for electrochemical analysis of HER2 using bioconjugate of GNR@Pd SSs—apt—HRP, Sensor. Actuator. B Chem. 296 (2019) 126650.

[49] L. Xu, W. Liang, Y. Wen, L. Wang, X. Yang, S. Ren, N. Jia, X. Zuo, G. Liu, An ultrasensitive electrochemical biosensor for the detection of mecA gene in methicillin-resistant Staphylococcus aureus, Biosens. Bioelectron. 99 (2018) 424–430, https://doi.org/10.1016/j.bios.2017.08.014.

[50] Y. Wen, H. Pei, Y. Shen, J. Xi, M. Lin, N. Lu, X. Shen, J. Li, C. Fan, DNA Nanostructure-based Interfacial engineering for PCR-free ultrasensitive electrochemical analysis of microRNA, Sci. Rep. 2 (2012) 14–18, https://doi.org/10.1038/srep00867.